Available online at www.sciencedirect.com
SCIENCE DIRECT®
Thermochimica Acta 405 (2003) 207–218
thermochimica acta
www.elsevier.com/locate/tca

Thermal activation of copper oxide based upon the copper hydrotalcites of the type $Cu_xZn_{6-x}Cr_2(OH)_{16}(CO_3)\cdot 4H_2O$

R.L. Frost*, Z. Ding

Inorganic Materials Research Program, School of Physical and Chemical Sciences, Queensland University of Technology, 2 George Street, GPO Box 2434, Brisbane, Qld 4001, Australia

Received 23 January 2003; received in revised form 12 March 2003; accepted 15 March 2003

Abstract

A combination of differential scanning calorimetry (DSC) and high-resolution differential thermogravimetric analysis (DTGA) coupled to a gas evolution mass spectrometer has been used to study the thermal properties of a chromium based series of Cu/Zn hydrotalcites of formulae $Cu_xZn_{6-x}Cr_2(OH)_{16}(CO_3)\cdot 4H_2O$ where x varied from 6 to 0.

The spacing for the $Cu_6Cr_2(OH)_{16}(CO_3)\cdot 4H_2O$ hydrotalcite is 6.95 Å which decreases to 6.69 Å with two moles of Zn substitution. The effect of cation substitution is small on the interlayer space. The variation was 0.26 Å. Crystallite size was found to be cation dependent. The larger sizes were observed for the zinc substituted hydrotalcites. It is observed that that the sum of the mass spectrometric curves of water and carbon dioxide matches precisely the differential thermogravimetric (DTG) curve. The effect of increased Zn composition results in the increase of the endotherms and weight loss steps to higher temperatures. Evolved gas mass spectrometry shows that water is lost in a number of steps and that the interlayer carbonate anion is lost simultaneously with hydroxyl units. Hydrotalcites in which M^{2+} consist of Cu, Ni or Co form important precursors for mixed metal-oxide catalysts. The application of these mixed metal oxides is in the wet catalytic oxidation of low concentrations of retractable organics in water. Therefore, the thermal behavior of synthetic hydrotalcites, $Cu_xZn_{6-x}Cr_2(OH)_{16}CO_3\cdot nH_2O$ was studied by thermal analysis techniques in order to determine the correct temperatures for the synthesis of the mixed metal oxides.

Keywords: Dehydration; Dehydroxylation; Hydrotalcite; Differential scanning calorimetry; High-resolution thermogravimetric analysis

1. Introduction

Much interest focuses on the use of nano-scale copper oxide for catalyst use [1–7]. The copper oxide may be used as a solid solution or as a mixture of mixed oxides [8–12]. The application of these mixed oxides is in environmental applications such as the catalytic oxidation of carbon monoxide and the wet oxidation of organics in aqueous systems. It is apparent that such metal-oxide mixtures may be obtained through the formation of hydrotalcites or double layered hydroxides. These nano-scale chemicals are produced through the thermal activation of copper salts such as copper carbonate, copper hydroxy-carbonate either synthetic or natural (malachite) and other copper salts for example copper nitrate. Equally well the thermally activated copper oxide materials may be obtained from the thermal activation of copper based hydrotalcites.

Hydrotalcites, or layered double hydroxides (LDH) are fundamentally anionic clays, and are less well known and more diffuse in nature than cationic

* Corresponding author.
E-mail address: r.frost@qut.edu.au (R.L. Frost).

0040-6031/$ – see front matter © 2003 Elsevier B.V. All rights reserved.
doi:10.1016/S0040-6031(03)00194-1

clays like smectites. The structure of hydrotalcite can be derived from a brucite structure ($Mg(OH)_2$) in which, e.g. Al^{3+} or Fe^{3+} (pyroaurite–sjögrenite) substitutes a part of the Mg^{2+} [13,14]. This substitution creates a positive layer charge on the hydroxide layers, which is compensated by interlayer anions or anionic complexes. In hydrotalcites a broad range of compositions are possible of the type $[M_{1-x}{}^{2+}M_x{}^{3+}(OH)_2][A^{n-}]_{x/n}{\cdot}yH_2O$, where M^{2+} and M^{3+} are the di- and trivalent cations in the octahedral positions within the hydroxide layers with x normally between 0.17 and 0.33. A^{n-} is an exchangeable interlayer anion. In this research, we are synthesizing copper based hydrotalcites of the general formulae $Cu_xZn_{6-x}Cr_2(OH)_{16}(CO_3){\cdot}4H_2O$ where x varies from 6 to 0. Whilst hydrotalcites based upon $Cu_xMg_{6-x}Al_2(OH)_{16}(CO_3){\cdot}4H_2O$ have been studied [5,15,16], it is apparent that the Cu/Zn based hydrotalcites with Cr as the trivalent cation have not. Importantly, the use of hydrotalcites in the synthesis of nanocomposites has enabled high temperature phase composite materials to be manufactured. Important to this work is the knowledge of when the hydrotalcite decomposes and the mechanisms for this decomposition. This decomposition temperature influences the temperature of the formation of this nanocomposite such that might be used for the photo-oxidation of organics in aqueous systems. This research compliments our studies in the synthesis and characterization of hydrotalcites. In this work, we report the high-resolution thermogravimetric analysis (TGA) of a series of hydrotalcites with different Cu and Zn.

2. Experimental

2.1. Synthesis of hydrotalcite samples

The hydrotalcites were synthesized by the co-precipitation method. Hydrotalcites with a composition of $Cu_xZn_{6-x}Cr_2(OH)_{16}(CO_3){\cdot}4H_2O$ and $Cu_xNi_{6-x}Cr_2(OH)_{16}CO_3{\cdot}nH_2O$ where x varied from 6 to 0, were synthesized. Two solutions were prepared, solution 1 contained 2 M NaOH and 0.125 M Na_2CO_3, solution 2 contained 0.75 M Cu^{2+} ($Cu(NO_3)_2{\cdot}6H_2O$) and 0.75 M Zn^{2+} ($Zn(NO_3)_2{\cdot}6H_2O$) (or 0.75 M Ni^{2+} ($Ni(NO_3)_2{\cdot}6H_2O$) together with 0.25 M Cr^{3+} (as ($Cr(NO_3)_3{\cdot}9H_2O$)). Solution 2 in the appropriate ratio was added to solution 1 using a peristaltic pump at a rate of 40 cm^3/min, under vigorous stirring, maintaining a pH of 10. To prepare hydrotalcites with different molecular formulae, the ratio of the Cu^{2+}/Zn^{2+} was varied according to the required formula. The precipitated minerals are washed at ambient temperatures thoroughly with water to remove any residual nitrate. The composition of the hydrotalcites was checked by ICP and ICP–AES analysis. The phase composition was checked by X-ray diffraction (XRD).

2.2. Thermal analysis

Thermal decomposition of the hydrotalcite was carried out in a TA® high-resolution thermogravimetric analyzer (series Q500) in a flowing nitrogen atmosphere (80 cm^3/min). The samples were heated in an open platinum crucible at a rate of 2.0 °C/min up to 500 °C. With the quasi-isothermal, quasi-isobaric heating program of the instrument the furnace temperature was regulated precisely to provide a uniform rate of decomposition in the main decomposition stage. The TGA instrument was coupled to a Balzers (Pfeiffer) mass spectrometer for gas analysis. Only selected gases were analyzed.

Differential scanning calorimetry (DSC) was performed on a TA® Instrument DSC Q10 analyzer. Sample powders were loaded into sealed alumina pan and heated to 500 °C at heating rate of 2 °C/min. The empty alumina pan was used as reference and the heat flow between the sample and reference pans was recorded.

2.3. X-ray diffraction

The temperature controlled XRD analyses were carried out on a Philips wide angle PW 3020/1820 vertical goniometer equipped with curved graphite-diffracted beam monochromators. The *d*-spacing and intensity measurements were improved by application of a self developed computer aided divergence slit system enabling constant sampling area irradiation (20 mm long) at any angle of incidence. The goniometer radius was enlarged from 173 to 204 mm. The radiation applied was Cu Kα from a long fine focus Cu tube, operating at 40 kV and 40 mA in stepscan mode with steps of 0.025° 2θ and a counting time of 1 s. Measured data were corrected with the Lorentz

polarization factor (for oriented specimens) and for their irradiated volume.

3. Results and discussion

3.1. X-ray diffraction analyses

The X-ray diffraction patterns of the $Cu_xZn_{6-x}Cr_2(OH)_{16}(CO_3)\cdot 4H_2O$ hydrotalcites are shown in Fig. 1. The patterns clearly show that the synthetic clays are layered structures. The sharp peaks in XRD patterns are accounted for by the presence of sodium nitrate. The samples were washed to remove the sodium nitrate before thermal analysis. Fig. 2 displays the variation in the peak position with the number of moles of zinc substitution into the hydrotalcite formulation. The spacing for the $Cu_6Cr_2(OH)_{16}(CO_3)\cdot 4H_2O$ hydrotalcite is 6.95 Å which decreases to 6.69 Å with two moles of Zn substitution. The effect of cation substitution is small on the interlayer space. The variation is 0.26 Å. The effect of cation substitution is small compared with variation in the size of the anion in the interlayer space. It has been shown that the spacing between the layers is controlled not by the cationic substitution into the hydrotalcite structure but rather by the size and concentration of the anions in the interlayer space [17].

Fig. 2 also displays the variation in peak width of the $d(0\,0\,1)$ peak. The peak width measures the crystal domain size of the hydrotalcite crystals according to the Scherrer equation.

$$L = \frac{\lambda K}{\beta \cos\theta}$$

where L is the mean crystallite dimension (in Å) along a line normal to the reflecting plane, K is a constant close to unity, and β is the width of the reflection at half height expressed in radians of 2θ. The peak width is 2.93° for the Cu only hydrotalcite decreases to 1.6° for the $Cu_4Zn_2Cr_2(OH)_{16}(CO_3)\cdot 4H_2O$ hydrotalcite increases to 2.58° for the $Cu_4Zn_2Cr_2(OH)_{16}(CO_3)\cdot 4H_2O$ hydrotalcite and has a value of 1.63° for the Zn only hydrotalcite. These values imply that the crystallite size is being determined by the cation substitution. Small crystallite sizes are found for the Cu hydrotalcites and large crystallite sizes for the zinc based hydrotalcites.

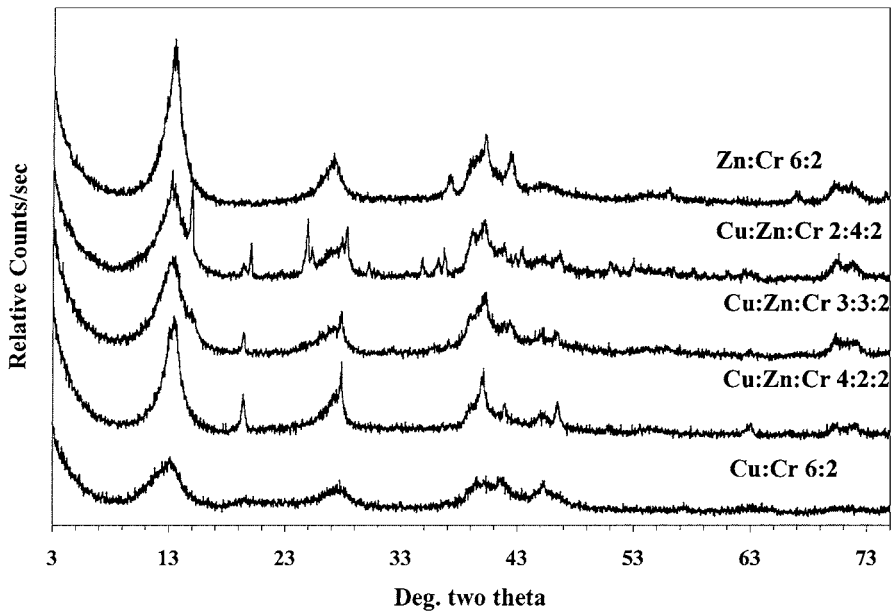

Fig. 1. X-ray diffraction patterns of the hydrotalcite $(Cu_xZn_{6-x})Cr_2(OH)_{16}(CO_3)\cdot 4H_2O$ as (a) $x = 6$, (b) $x = 4$, (c) $x = 3$, (d) $x = 2$, (e) $x = 0$.

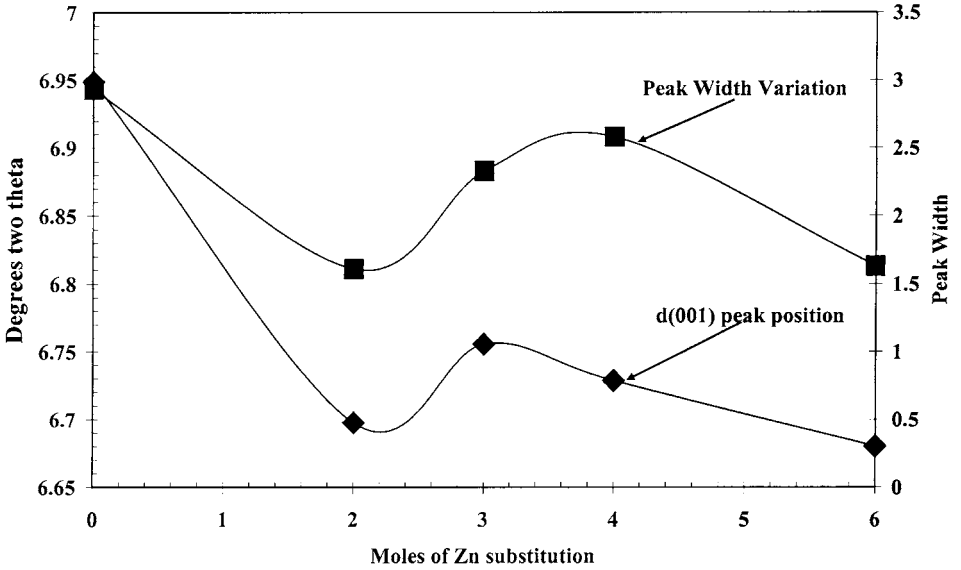

Fig. 2. Variation in the peak position and peak width with moles of zinc substitution.

3.2. High-resolution thermogravimetric analysis and mass spectrometric analysis

The differential thermogravimetric (DTG) analysis curves together with the mass spectrometric analysis curves are shown in Fig. 3. The results of the integral of the DTG curves as determined by the band component analysis of the DTG curves are reported in Table 1. Each peak in the DTG curve represents a weight loss step and the total weight loss step is 100%. Such a table is somewhat arbitrary but does allow some classification of the weight loss steps. The results of the mass spectrometric analyses are provided in Table 2. The DTG curves are divided into weight loss steps according to the band component analysis. These steps correspond to the maxima in the DTG curves. The weight loss steps are further categorized according to the actual temperature of the weight loss. Broadly speaking there are seven weight loss steps as determined by the temperature of the weight loss.

The DTG pattern for the synthesized hydrotalcites appears different for each of the synthesized hydrotalcites. Some similarity exists between the two end members of the hydrotalcite series namely

Table 1
Results of the DTG for Cu/Zn/Cr hydrotalcites

Weight loss step	Cu/Zn (temperature, % weight loss)				
	6/0	4/2	3/3	2/4	0/6
1		89.4, 15.8	85.7, 7.3	90.7, 8.4	73.6, 14.1
2	100.5, 23.9				112.3, 16.9
3	143.5, 26.5	149.3, 13.0		138.1, 4.8	
4	165.2, 5.6	158.8, 7.0	157.5, 14.5	154.0, 3.4	
5	190.0, 33.2	180.1, 11.1	178.9, 3.2	198.2, 60.2	215.0, 38.0
6	338.4, 7.2	207.9, 45.0	206.3, 47.8	274.0, 22.8	254.0, 30.8
7	387.0, 2.6	409.4, 1.3	252.0, 21.1		
8			294.0, 5.3		

$Cu_6Cr_2(OH)_{16}(CO_3)\cdot 4H_2O$ and $Zn_6Cr_2(OH)_{16}(CO_3)\cdot 4H_2O$. When the mixed Zn–Cu hydrotalcites are formed some similarity exists as well. The question arises as to why the thermal behavior of the hydrotalcite series is different. In brucite type solids, there are tripod units M_3OH with several metal cations such as M, M′, M″. In hydrotalcites such as those based upon Cu and Zn of formula $Cu_xZn_{6-x}Cr_2(OH)_{16}(CO_3)\cdot 4H_2O$, a number of statistical permutations of the M_3OH units are involved. These are Cu_3OH, Zn_3OH, Cr_3OH and combinations such as Cu_2ZnOH, Zn_2CuOH, Cu_2CrOH, Cr_2CuOH, Cr_2ZnOH, Zn_2CrOH, and even CuZnCrOH. These types of units will be distributed according to a

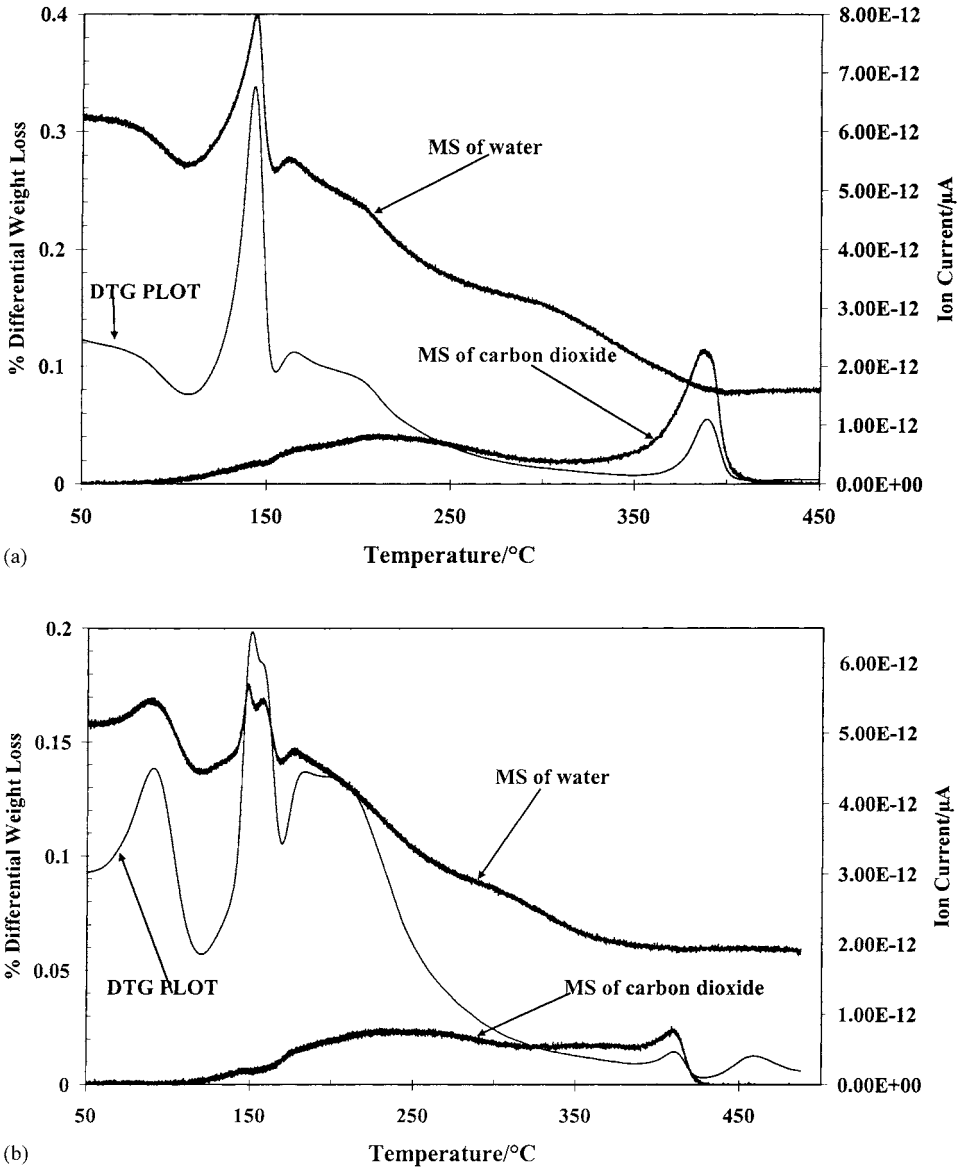

Fig. 3. Differential weight loss and MS of water and carbon dioxide for the hydrotalcites $(Cu_xZn_{6-x})Cr_2(OH)_{16}(CO_3)\cdot 4H_2O$ as (a) $x = 6$, (b) $x = 4$, (c) $x = 3$, (d) $x = 2$, (e) $x = 0$.

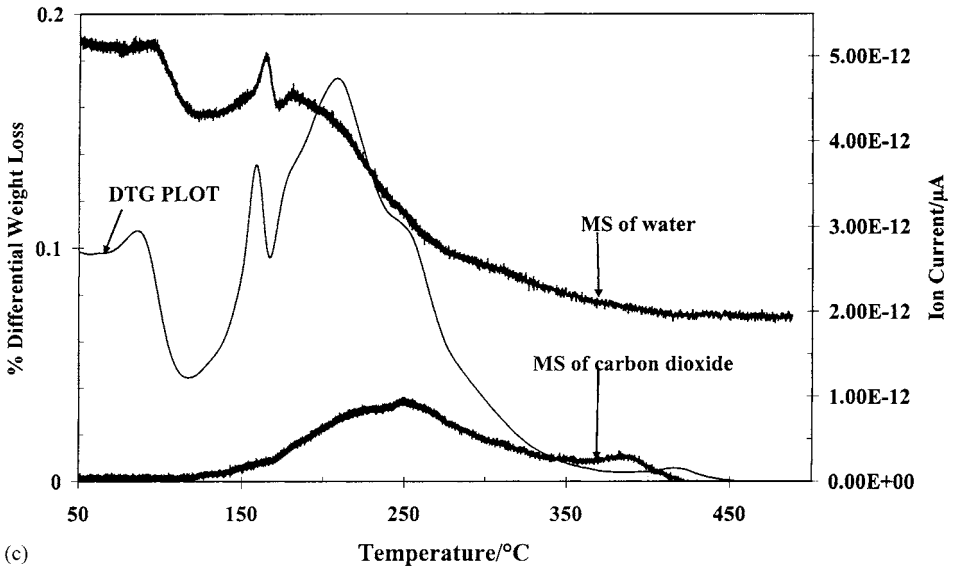

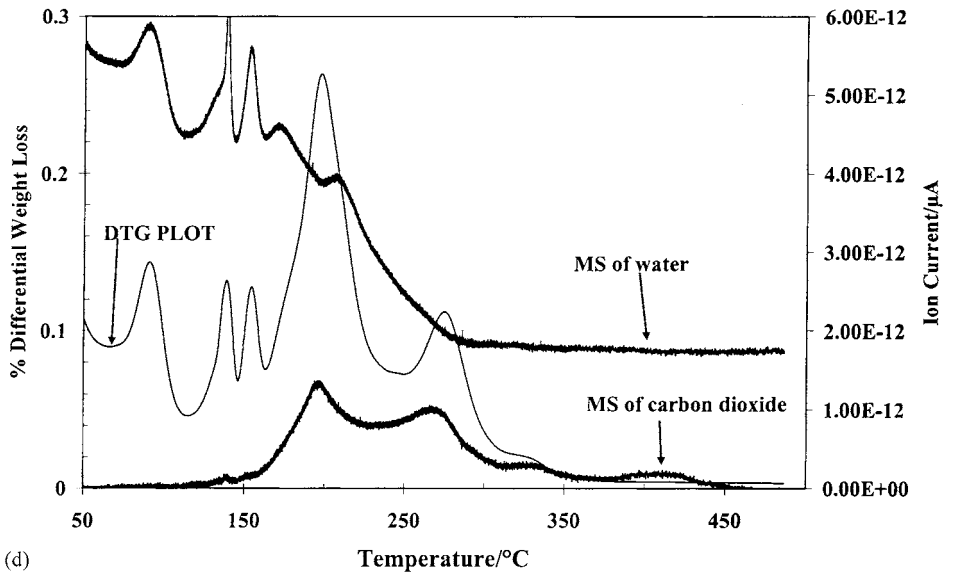

Fig. 3. (*Continued*).

probability distribution according to the composition. In this model, a number of assumptions are made, namely that the molecular assembly is random and that no islands or lakes of cations are formed. Such assembly is beyond the scope of this work but needs to be investigated [18]. Insight into the unique structure of hydrotalcites has been obtained using a combination of infrared spectroscopy [18]. The hydroxyl-stretching units of CuOH, ZnOH and CrOH, are identified by unique band positions. The identification of unique bands or lack thereof for these units makes it possible to assess whether there is a unique and regular arrangement of cations in the hydrotalcite structure. It is proposed that for $Cu_xZn_{6-x}Al_2(OH)_{16}(CO_3)\cdot 4H_2O$

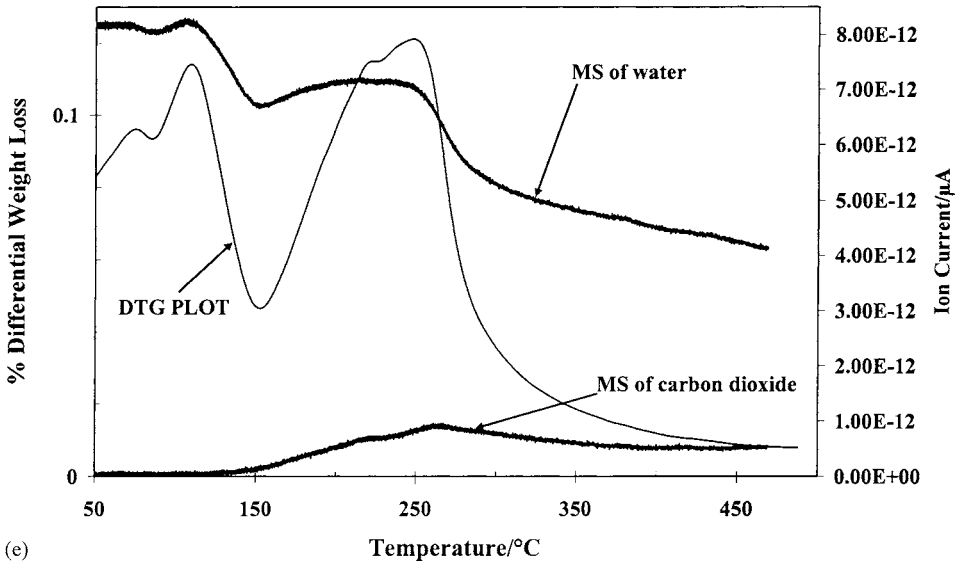

Fig. 3. (*Continued*).

hydrotalcites when x is less than or equal to two, that the cations are randomly assembled. However, when $x = 3$, separate bands for each of the cationic hydroxyls can be identified. This means that 'lakes' or 'islands' of the cations are formed in the hydrotalcite structures. It is suggested that a similar result would be obtained for the chromium based hydrotalcites.

In the simplest case namely $Cu_6Cr_2(OH)_{16}(CO_3)\cdot 4H_2O$ the types of units would be Cu_3OH, Cu_2CrOH, $CuCr_2OH$ and Cr_3OH. A similar situation would exist for the $Zn_6Cr_2(OH)_{16}(CO_3)\cdot 4H_2O$ hydrotalcite. In a somewhat oversimplified model, for the $Cu_6Cr_2(OH)_{16}(CO_3)\cdot 4H_2O$ hydrotalcite, the principal dehydroxylation weight loss steps would be due to the Cu_3OH and Cr_3OH bands. It is possible that the dehydroxylation steps are cation dependent based on the bond strength of the OH unit bonded to the cation. For the $Cu_6Cr_2(OH)_{16}(CO_3)\cdot 4H_2O$ hydrotalcite, there are four principal weight loss steps: (a) loss of water in the 75–100 °C temperature range, (b) loss of hydroxyls from the Cu_3OH and Cr_3OH units as well as the mixed cationic species, (c) loss of carbonate and water simultaneously and (d) loss of carbonate only. For this hydrotalcite, the loss of the hydroxyl units occurs over a very sharp temperature range namely 122–156 °C. What is extremely important in Fig. 3a–e is the observation that the sum of the mass spectrometric curves of water and carbon dioxide matches precisely the DTG curve. Step (c) above appears to be over a wide range of temperatures from 156 to 220 °C. This indicates the water from the dehydroxylation of the hydrotalcite surface and carbon dioxide are lost simultaneously. The step (d) occurs at around 390 °C. The carbon dioxide originates from the carbonate anions in the interlayer. A similar analysis may be made for the $Zn_6Cr_2(OH)_{16}(CO_3)\cdot 4H_2O$ hydrotalcite, where the same four weight loss steps may be observed: (a) loss of water over the 50–90 °C temperature range, (b) loss of OH units through dehydroxylation over the 100–180 °C temperature range and (c) loss of water and carbonate over the 160–300 °C temperature range. Step (d) appears to be absent for the $Zn_6Cr_2(OH)_{16}(CO_3)\cdot 4H_2O$ hydrotalcite. This suggests a different mechanism for decomposition for this hydrotalcite compared with that of the $Cu_6Cr_2(OH)_{16}(CO_3)\cdot 4H_2O$ hydrotalcite.

The thermal behavior of the mixed Cu/Zn hydrotalcites appears different from that of the end members. Additional weight loss steps are observed. In Fig. 3b and d two weight loss steps are clearly observed over the 137–174 °C temperature range for the $Cu_4Zn_2Cr_2(OH)_{16}(CO_3)\cdot 4H_2O$ hydrotalcite and over the 130–164 °C temperature range for the $Cu_2Zn_4Cr_2(OH)_{16}(CO_3)\cdot 4H_2O$ hydrotalcite. The

Table 2
Results of the MS for Cu/Zn/Cr hydrotalcites

Mass loss step	Cu/Zn (temperature, % mass loss)									
	6/0		4/2		3/3		2/4		0/6	
	H_2O	CO_2	H_2O	CO_2	H_2O	CO_2	H_2O	CO_2	H_2O	CO_2
1	134.5, 30.7		88.7, 20.9		91.2, 16.2		91.8, 15.1		75.5, 4.0	
2	143.5, 17.6		148.2, 19.3		162.2, 29.2		130.5, 5.7		111.8, 23.7	
3	163.2, 7.6		158.2, 7.75		184.0, 8.4		138.3, 13.2		205.6, 39.0	205.9, 7.3
4	188.0, 32.1	216, 61.3	180.4, 5.6		205.0, 46.3	216.0, 24.4	152.5, 13.0		248.8, 33.2	269.5, 92.6
5	307.4, 11.9		197.8, 44.76	200.6, 14.7	250.0, 0.5		172.7, 17.6	196.0, 40.7		
6			309.2, 1.6	265.0, 58.7		261.0, 69.1	188.9, 4.7			
7							208.6, 30.5	261.6, 47.8		
8		387.0, 38.0		373.0, 23.7		381.0, 6.4		333.0, 5.3		
9				407.0, 2.9				401.0, 6.2		

same additional weight loss steps are observed for the $Cu_3Zn_3Cr_2(OH)_{16}(CO_3)\cdot 4H_2O$ hydrotalcite in the 140–190 °C temperature range except that the second steps is somewhat masked by the weight loss step of the carbonate–water step (step (c)). It is proposed that the observation of the two additional steps may be attributed to the loss of hydroxyl units from the different cations in the structure. If this is the case then thermal analysis is providing information on molecular assembly and that the cations are not randomly distributed but are forming lakes of cations in the structure.

All of the zinc containing hydrotalcites all show a weight loss step in the 75–90° temperature range. This weight loss step was not observed for the Cu–Cr hydrotalcite, although a weight loss step is observed at 100.5 °C. This weight loss step is attributed to adsorbed water. The weight loss varies from 7.3 to 15.8%. The principle weight loss step for the Cu–Cr hydrotalcite is at 100.5 °C where a weight loss of 23.9% is observed. A second weight loss step is observed for the $Cu_6Cr_2(OH)_{16}(CO_3)\cdot 4H_2O$ hydrotalcite at 143.5° with a 26.5% weight loss. For the $Cu_4Zn_2Cr_2(OH)_{16}(CO_3)\cdot 4H_2O$ and the $Cu_2Zn_4Cr_2(OH)_{16}(CO_3)\cdot 4H_2O$ hydrotalcites weight loss steps are also observed at 149.3 and 138.1 °C with 13.0 and 4.8% weight loss. For these two hydrotalcites there appears to be two closely overlapping steps at 149 and 158 °C, and 138 and 154 °C. Also for the $Cu_3Zn_3Cr_2(OH)_{16}(CO_3)\cdot 4H_2O$ hydrotalcite there are two weight losses at 157 and 178 °C. The question arises as to why we do not observe these two close weight loss steps for the $Cu_6Cr_2(OH)_{16}(CO_3)\cdot 4H_2O$ and $Zn_6Cr_2(OH)_{16}(CO_3)\cdot 4H_2O$ hydrotalcites. It is possible that the weight loss steps are attributable to the loss of hydroxyl units from individual cations. For example, for the $Cu_4Zn_2Cr_2(OH)_{16}(CO_3)\cdot 4H_2O$ hydrotalcite two weight loss steps are observed at 149.3 and 158.8 °C with weight losses of 13.0 and 7.0%. The ratio of the two weight loss steps is approximately 2/1. The ratio of the two weight loss steps is approximately 2/1. This may be an observation of molecular assembly of the Zn and Cu as measured by thermogravimetric analysis.

For the $Cu_4Zn_2Cr_2(OH)_{16}(CO_3)\cdot 4H_2O$ hydrotalcite there is a third dehydroxylation step with a weight loss of 11.1% at 180.1 °C. The mass spectrometric curves (MS) indicate that both water and CO_2 are being detected at this weight loss step. For this hydrotalcite, two further weight loss steps are observed at 207.9 and 409.4 °C with weight losses of 15.0 and 1.3%. The MS data shows that these weight loss steps are ascribed to the loss of carbonate anion from the interlayer.

The mass spectrometric curves of evolved gases namely water vapor and carbon dioxide are also shown in Fig. 3. The figure clearly shows the MS of the evolved gases as a function of temperature. What may be clearly distinguished is that: (a) initially water vapor is measured only, (b) there is a temperature range where the evolved gases are water vapor and carbon dioxide and (c) a temperature interval over which carbon dioxide is evolved only. The mass spectra were analyzed by band resolution on the assumption that the total mass gain is 100% for each of water vapor and carbon dioxide. The results are reported in Table 2. The MS of nitric oxide and nitrogen dioxide, the possible by-products of the thermal decomposition of nitrate was also measured but no mass spectrum was obtained, thus indicating the absence of nitrate in the interlayer space. Fig. 3 clearly shows the fundamental principal that the addition of the mass spectrometric curves follows the DTG curve with absolute precision. This means that a direct comparison can be made between the DTG results and the mass spectrometric results.

The mass loss of water for the $Cu_6Cr_2(OH)_{16}(CO_3)\cdot 4H_2O$ hydrotalcite at 134.5 °C is 30.7% which may be compared with the weight loss step of 26.5% for the DTG step at 143.5 °C. It must be kept in mind that the precision of the DTG results will be significantly greater than that obtained by the MS results. Similarly, the weight loss step at 165.2 °C of 5.6% may be compared with the mass loss of 7.6% at 163.2 °C in the MS data. The weight loss step 5 at 190 °C for this hydrotalcite must be compared with the sum of the evolved masses of both water and carbon dioxide. The mass gain of carbon dioxide at 387 °C is directly comparable to the weight loss step 7. In this step CO_2 is being evolved only. These results prove that there is excellent correspondence between the weight loss steps and the mass gain of evolved gases. Such excellent correspondence is evident for the other hydrotalcites as is evidenced by the comparison of the data in Tables 1 and 2.

3.3. Differential scanning calorimetry

Each of the Cu/Zn chromium based hydrotalcites was measured by differential scanning calorimetry, the

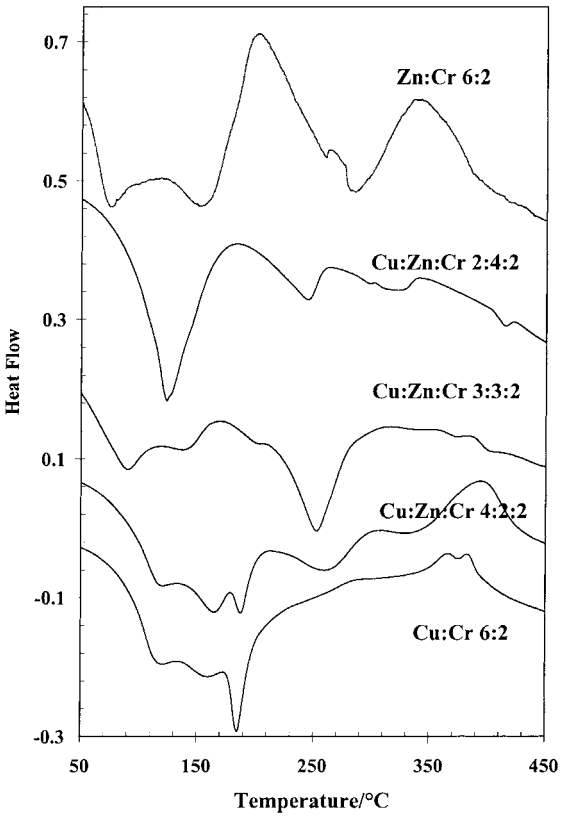

Fig. 4. DSC of the hydrotalcites $(Cu_xZn_{6-x})Cr_2(OH)_{16}(CO_3)\cdot 4H_2O$ as (a) $x = 6$, (b) $x = 4$, (c) $x = 3$, (d) $x = 2$, (e) $x = 0$.

scans of which are shown in Fig. 4 and the results in Table 3. Fundamentally, there is no relationship between the DSC results and the DTG or MS results. This is not unexpected since DSC is measuring the heat flow properties, which bares little relationship to the weight loss or evolved gas mass gain properties. Further the rates of heating and the experimental programs are different between the two techniques. Seven heat flow steps are identified. Heat flow step 1 is attributed to the thermal energy required to remove the adsorbed water. Water may be present as a means of hydrating the anion in this case the carbonate anion. Up to 52.4% of the total heat flow is required to remove the water from the hydrotalcite.

Heat flow steps 2 and 3 are probably associated with dehydroxylation. The value of the heat flow step varies from 20.6 to 23.4%. The value for the Cu_2Zn_4 hydrotalcite appears out of step. Heat flow steps 4 and 5 are associated with the loss of carbon dioxide. Heat flow steps 6 and 7 are minor.

Recent studies of a complex hydrotalcite based upon Cu/Co/Zn/Al layered double hydroxides with various Cu/Co atom ratios showed that using thermal analyses of materials indicated three stages of endothermic weight loss processes due to the loss of interlayer H_2O and some loosely bound CO_3^{2-} (100–250 °C), loss of structural H_2O and CO_3^{2-} (250–400 °C) and the loss of some strongly held CO_3^{2-} anions (above 500 °C) [12]. These results are in good agreement with our data. Other work has shown that for Cu/Zn/Co/Cr hydrotalcites the thermal analysis results were independent of the cation [7]. Such a concept is different to what has been reported in this research. Here, we find that the thermal analyses both DSC and differential thermogravimetric analysis (DTGA) coupled to MS are cation dependent and that the thermal analysis steps are cation mole ratio dependent.

The authors recently published data on the Cu/Zn/Al hydrotalcite system [19]. A series of $Cu_{6-x}Zn_xAl_2(OH)_{16}(CO_3)\cdot 4H_2O$ hydrotalcites with

Table 3
Results of the DSC for Cu/Zn/Cr hydrotalcites

Heat flow step	Cu/Zn (temperature, % heat flow)				
	6/0	4/2	3/3	2/4	0/6
1	116, 22.0	120, 25.6	88.7, 39.2	124, 52.4	96.5, 48.1
2	156, 20.6	164, 23.4	156.5, 20.7		158, 21.6
3	185, 9.4	188, 5.2			
4		208, 4.6	207.3, 6.8	228.7, 6.5	
5	272, 37.8	260, 30.3	252, 31.6	245, 34.7	291, 30.3
6	326, 5.5	337, 11.0	371, 0.4	303, 3.7	
7	375, 0.5		403, 1.2	323, 2.2	

zinc substitution were studied by a combination of differential scanning calorimetry and high-resolution thermogravimetry in combination with an evolved gas mass spectrometer. The results of the DSC showed that increased substitution of the Cu by Zn results in the shift of the heat flow steps to higher temperature. In contrast, DSC of the chromium hydrotalcites resulted in a shift of the heat flow steps to lower temperatures. This difference may be due to the cation avoidance rule which states that trivalent cations sharing octahedral edges exert a mutual repulsion which may be a dominant force in hydrotalcite structures [20]. Studies of Cu/Zn with either Al or Cr hydrotalcites have been few; however there have been some studies with Ni involving either Al of Cr [3].

Previous studies of mixed Ni/Cr and Ni/Al hydrotalcites using X-ray diffraction and infrared spectroscopic analyses, have shown the level of supersaturation and/or a following hydrothermal treatment influence only the crystallinity of the precipitates, but do not modify their nature or the characteristics of the mixed oxides obtained by thermal decomposition [3]. The TG and DSC analyses of the hydrotalcites showed that their decomposition involved an initial loss of the interlayer H_2O followed by elimination of the carbonates and hydroxide ions, with some differences directly related to the crystallinity of the samples. The Ni/Al samples obtained by thermal decomposition are more stable than the Ni/Cr samples. For all the samples investigated, the formation of a spinel phase has a neg. effect, giving rise to remarkable increases in both NiO crystal size and reducibility. The thermal stability of the NiO particles obtained by decomposition of Ni/Al hydrotalcite seems to be related mainly to the nature of the trivalent ion present and, as a consequence, so is the behavior of the oxide obtained by thermal decomposition. Other studies based upon Ni/Al hydrotalcites suggest that the trivalent cation is important in the thermal stability of the NiO [4].

The endotherms are complex with overlapping endothermic steps suggesting that some cation ordering occurs in the hydrotalcite structure. More steps are observed in the DSC patterns than in the DTGA patterns. It was proposed that some of the endothermic steps are surface phase related involving changes in the hydroxyl surface structure. High-resolution DTGA combined with mass spectrometry shows that the temperature of the dehydroxylation of the $Cu_{6-x}Zn_xAl_2(OH)_{16}(CO_3)\cdot 4H_2O$ hydrotalcite increases with increased Zn composition. Such hydrotalcites have the potential for low temperature methanol synthesis [21]. Such hydrotalcites may also be useful for toluene oxidation [5]. The zinc oxide may serve as a promoter of the copper oxide in the oxidation process.

4. Conclusions

A series of $(Cu_xZn_{6-x})Cr_2(OH)_{16}(CO_3)\cdot 4H_2O$ hydrotalcites with zinc substitution have been studied by a combination of differential scanning calorimetry and high-resolution thermogravimetry in combination with an evolved gas mass spectrometer. DSC shows that increased substitution of the Cu by Zn results in the shift of the heat flow steps to lower temperature. The endotherms are complex with overlapping peaks suggesting that some cation ordering occurs in the hydrotalcite structure. More steps are observed in the DSC patterns than for the DTGA. This suggests that some of the endothermic steps are surface phase related involving changes in the hydroxyl surface structure. High-resolution DTGA combined with mass spectrometry shows that the temperature of the dehydroxylation of the hydrotalcite decreases with increased Zn composition. Four principal weight loss steps are observed: (a) loss of adsorbed water in the 40–50 °C temperature range, (b) loss of water between 110 and 150 °C, (c) dehydroxylation in the 200–248 °C temperature range and (d) loss of carbonate in the 300–350 °C temperature range.

The importance of this work rests with the ability to make mixed oxides at the atomic level. In this case mixed oxides of Cu, Zn and Cr are formed. Controlled heating results in oxide formation. Heating to too high a temperature will result in the formation of chromates. Both zinc oxide and copper oxide can act as photocatalysts. The presence of the mixed oxides, mixed at the atomic level, can enhance their catalytic activity.

References

[1] M.D. Arco, V. Rives, R. Trujillano, Stud. Surf. Sci. Catal. 87 (1994) 507.
[2] C. Barriga, J.M. Fernandez, M.A. Ulibarri, F.M. Labajos, V. Rives, J. Solid State Chem. 124 (1996) 205.

[3] O. Clause, M. Gazzano, F. Trifiro, A. Vaccari, L. Zatorski, Appl. Catal. 73 (1991) 217.
[4] O. Clause, B. Rebours, E. Merlen, F. Trifiro, A. Vaccari, J. Catal. 133 (1992) 231.
[5] F. Kovanda, K. Jiratova, J. Rymes, D. Kolousek, Appl. Clay Sci. 18 (2001) 71.
[6] F.M. Labajos, V. Rives, Inorg. Chem. 35 (1996) 5313.
[7] P. Porta, S. Morpurgo, Appl. Clay Sci. 10 (1995) 31.
[8] K.K. Rao, M. Gravelle, J.S. Valente, F. Figueras, J. Catal. 173 (1998) 115.
[9] V. Rives, A. Dubey, S. Kannan, Phys. Chem. Chem. Phys. 3 (2001) 4826.
[10] V. Subramani, S. Hashimoto, N. Satoh, K. Suzuki, T. Mori, Prepr. Am. Chem. Soc., Div. Pet. Chem. 46 (2001) 17.
[11] E.H. Van Broekhoven, European Patent Application (AKZO N.V., Neth.) Ep, 1988, 16 pp.
[12] S. Velu, K. Suzuki, S. Hashimoto, N. Satoh, F. Ohashi, S. Tomura, J. Mater. Chem. 11 (2001) 2049.
[13] L. Hickey, J.T. Kloprogge, R.L. Frost, J. Mater. Sci. 35 (2000) 4347.
[14] J. Theo Kloprogge, R.L. Frost, Phys. Chem. Chem. Phys. 1 (1999) 1641.
[15] E. Kanezaki, K. Kinugawa, Y. Ishikawa, Chem. Phys. Lett. 226 (1994) 325.
[16] Y. Kobayashi, T. Honna, T. Katamoto, A. Yamamoto, Jpn. Kokai Tokkyo Koho (Toda Kogyo Corp., Japan) Jp, 2000, 8 pp.
[17] J.T. Kloprogge, D. Wharton, L. Hickey, R.L. Frost, Am. Mineral. 87 (2002) 623.
[18] R.L. Frost, Z. Ding, W.N. Martens, T.E. Johnson, J.T. Kloprogge, Spectrochim. Acta, Part A: Mol. Biomol. Spectrosc. 59A (2003) 321.
[19] R.L. Frost, Z. Ding, W.N. Martens, T.E. Johnson, Thermochim. Acta 398 (2003) 167.
[20] E.W. Radoslovitch, Am. Mineral. 48 (1963) 76.
[21] R.H. Hoeppener, E.B.M. Doesburg, J.J.F. Scholten, Appl. Catal. 25 (1986) 109.